

Nuclear binding energies from moment methods: Harmonic oscillator Hamiltonian

F. J. Margetan, A. Klar, and J. P. Vary

Ames Laboratory—Department of Energy and Department of Physics, Iowa State University, Ames, Iowa 50011

(Received 29 March 1982)

Total binding energies for systems of N neutrons and Z protons near $N=Z=8$ are obtained for the harmonic oscillator Hamiltonian via moment methods and are compared with the exact results. We examine the accuracy of employing only the few lowest moments of the eigenvalue density to predict the ground state (g.s.) energy as a function of several ingredients in the method. We find systematic errors are strongly dependent on the scheme chosen for truncating the single particle space and rather weakly dependent on the size of the model space in many cases of interest. Two functional forms approximating the exact eigenvalue distribution, the Gram-Charlier series and the Weibull distribution, give results of comparable accuracy in cases where three moments are employed. Best overall accuracy is obtained using the traditional truncation scheme where all single particle states below a fixed energy are retained. For this truncation scheme, the distribution of energy eigenvalues is significantly skewed. However, the Gaussian approximation, which requires only the two lowest moments, yields one of the better estimates of the g.s. energy. This is true for both the total distribution of eigenvalues and for the distribution restricted to states of specific total angular momentum. The absolute error in the g.s. energy estimate is generally found to grow with increasing model space size; however, most of the error is systematic, and the *relative* binding energies of adjacent nuclei are found to be predicted with considerably greater accuracy. Isolation of these systematic errors plus demonstration of small errors in relative energies enhances the prospects for obtaining reliable total nuclear binding energies from realistic (no-core) Hamiltonians using moment methods.

NUCLEAR STRUCTURE Binding energies from moment methods; spectral properties of harmonic oscillator Hamiltonian; efficacy of moment methods versus truncation scheme and model space size.

I. INTRODUCTION

Spectral properties of nuclei have long been investigated in the shell model where an effective Hamiltonian is diagonalized in a finite model space. Owing to computer limitations, the dimensionality of the many particle model space is limited to about 10^5 states. On the other hand, realistic Hamiltonians often display strong coupling to states outside these limited model spaces. Furthermore, it is well known that "intruder states," i.e., states whose parentage is primarily outside the model space, exist already in the low-lying spectra of nuclei. These deficiencies motivate the development and testing of methods which can yield the spectral properties of nuclei in much larger model spaces. One promising approach is the moment method which begins with the calculation of the moments of the eigenvalue distribution function.¹⁻⁴ Then, one generates a smooth function with the same lowest moments as the exact eigenvalue distribution and uses this function to study the spectral properties of nuclei. As an example of the increase in model space size which

the moment method makes possible, we perform calculations in this work for model spaces up to a dimensionality of 10^{33} many-body states.

Previous efforts⁵⁻⁷ have provided good evidence that the methods work well in small model spaces with realistic effective Hamiltonians where exact diagonalizations could be performed for comparison. Our primary goal here is to test moment methods in large model spaces. Such a test requires a soluble Hamiltonian so that the exact energy spectrum may be compared with the moment method estimate. In addition the solution of the soluble problem should mirror a large shell model diagonalization as closely as is practical. In the present test we investigate the accuracy of the moment method in predicting the ground state (g.s.) energy of the harmonic oscillator Hamiltonian. Although this soluble Hamiltonian lacks the strong two-body interaction present in the realistic case, the test problem is quite close in spirit and detail to nuclear shell model calculations which often employ harmonic oscillator eigenfunctions as an expansion basis. Some of the model spaces and other calculational ingredients studied here have

been^{7,8} and will be⁹ employed in applications with realistic Hamiltonians. With the present study we identify some of the strengths and weaknesses of the moment method which should characterize the accuracy of large-basis realistic applications.

The organization of the paper is as follows. Section II summarizes our notation and reviews the calculational method. In Sec. III we describe the properties of the density of states (DOS) function for the finite space treatment of the harmonic oscillator Hamiltonian. Our main study of the error in the Ratcliff estimate⁵ of the ground state energy is presented in Sec. IV. There we examine the dependence of absolute and relative errors on truncation scheme, basis size, number of moments employed (up to four), and choice of the smooth approximation to the DOS function. Our principal investigations use moments of the *total* DOS function to estimate the g.s. energy. However, at the end of Sec. IV we also apply the moment method to basis spaces of fixed total angular momentum. We conclude in Sec. V with a summary of our findings and their consequences for calculations with realistic nuclear Hamiltonians.

II. BINDING ENERGIES FROM MOMENTS

We employ the soluble one-body harmonic oscillator Hamiltonian to describe states of A nucleons with N neutrons and Z protons:

$$H_0 = \sum_{k=1}^{A=N+Z} \left\{ \frac{\vec{p}_k^2}{2m} + \frac{1}{2} m \omega^2 |\vec{x}_k|^2 \right\} \\ = \sum_{\alpha} (N_{\alpha} + \frac{3}{2}) \hbar \omega_{\alpha} a_{\alpha}^{\dagger} a_{\alpha}, \quad (1)$$

where a_{α}^{\dagger} and a_{α} represent the fermion creation and destruction operators, respectively. Here α represents a list of quantum numbers $(n, l, s = \frac{1}{2}, j, m_j, t = \frac{1}{2}, t_z)$ specifying the number of radial nodes, the orbital, spin and total angular momenta, the angular momentum projection, the isospin, and the isospin projection, respectively. The energy label N_{α} occurring in Eq. (1) is given by $N_{\alpha} = 2n + l$. A normalized, totally antisymmetric eigenstate of H_0 is written

$$|\phi_i\rangle = a_{\alpha_1}^{\dagger} a_{\alpha_2}^{\dagger} \dots a_{\alpha_N}^{\dagger} a_{\alpha_1}^{\dagger} a_{\alpha_2}^{\dagger} \dots a_{\alpha_Z}^{\dagger} |0\rangle, \quad (2)$$

where $|0\rangle$ is the vacuum, and where the α_k and the α'_k refer to neutron ($t_z = -\frac{1}{2}$) and proton ($t_z = \frac{1}{2}$) states, respectively. In practice one requires that the set of $|\phi_i\rangle$ employed as an expansion basis be made finite. Traditionally, this is accomplished by designating a finite number of the single-particle (sp) states as "active," and then restricting the α_k and α'_k

in Eq. (2) to the active group. If there are d active single-nucleon states for each of $t_z = \pm \frac{1}{2}$, then the number of distinct $|\phi_i\rangle$ in the truncated basis is

$$D = \binom{d}{N} \binom{d}{Z} \quad (3)$$

and

$$P \equiv \sum_{i=1}^D |\phi_i\rangle \langle \phi_i| \quad (4)$$

projects onto the many-nucleon subspace spanned by this basis. Two truncation schemes are used in the present work. In the energy truncation scheme (ETS), the active single-nucleon states are defined as those having energy label $N_{\alpha} = (2n + l) \leq N_E$, where the cutoff value may range over $1 \leq N_E \leq 9$. The symmetric truncation scheme (STS) uses a triangular grouping of active orbits centered about $N_{\alpha} = N_S$, where $1 \leq N_S \leq 7$ for the calculations described in Secs. III and IV. For the STS, every sp state with $N_{\alpha} \leq N_S$ is active, and, in addition, each state with $N_{\alpha} < N_S$ has an active companion state with the same (l, s, j, m_j, t, t_z) quantum numbers but with $N'_{\alpha} = 2N_S - N_{\alpha}$. For example, when $N_S = 2$, the active orbits of the STS basis include $nl_j = 1P_{1/2}$, $1P_{3/2}$, and $2S_{1/2}$ in addition to all sp orbits having $N_{\alpha} \leq 2$. We refer to a truncated expansion basis

$$\{ |\phi_i\rangle; i = 1, 2, \dots, D \}$$

by its type (S for STS, E for ETS) and by the integer d . For example, $E112$ denotes an energy truncated basis employing 112 single-neutron and 112 single-proton states. Note that a closed core is not assumed when constructing the truncated basis. This "no-core" basis is motivated by the desire to obtain total binding energies of nuclei in future applications with realistic Hamiltonians.⁹

Approximate eigenstates and eigenvalues of a nuclear Hamiltonian, H , may be obtained by diagonalizing the matrix

$$\{ \langle \phi_i | H | \phi_{i'} \rangle; i, i' = 1, 2, \dots, D \}$$

whose eigenvectors correspond to exact eigenstates of PHP . We use $|\psi_m\rangle$ to denote an energy-ordered eigenstate of PHP :

$$PHP |\psi_m\rangle = E_m |\psi_m\rangle, \quad m = 1, 2, \dots, D, \quad (5)$$

$$E_{g.s.} \equiv E_1 \leq E_2 \leq \dots \leq E_D.$$

E_m is a rigorous upper bound to the m th energy-ordered eigenvalue of H , and approaches the latter monotonically as the expansion basis is enlarged.¹⁰ We use

$$\rho(E) = \sum_{m=1}^D \delta(E - E_m) \quad (6)$$

to denote the density-of-states (DOS) distribution which would result from the diagonalization of PHP in the finite basis.

In cases where $D \gtrsim 10^5$ and the partial or complete diagonalization of the PHP matrix is impractical, one may obtain characteristics of the PHP spectrum by using moment methods. One first approximates

$\rho(E)$ by a continuous function $\rho_a(E)$ having the same total integral and first few moments as $\rho(E)$. Estimates of specific PHP spectral properties, such as the g.s. energy, are then obtained from ρ_a . This program requires exact moments of $\rho(E)$, which can be found from

$$\langle E^p \rangle \equiv \frac{1}{D} \int_{-\infty}^{\infty} \rho(E) E^p dE = \frac{1}{D} \sum_{m=1}^D (E_m)^p = \frac{1}{D} \sum_{m=1}^D \langle \psi_m | (PHP)^p | \psi_m \rangle = \frac{1}{D} \sum_{i=1}^D \langle \phi_i | (PHP)^p | \phi_i \rangle. \quad (7)$$

The last equality utilizes the invariance of a matrix trace under a unitary transformation. The term on the far right-hand side (rhs) of Eq. (7) can be rewritten in terms of the elementary matrix elements of H by using the trace reduction techniques of Ginocchio and Ayik.^{2,3,11} For our present effort we need consider only the situation where H is diagonal in the expansion basis:

$$\langle 0 | a_\alpha H a_\beta^\dagger | 0 \rangle = \epsilon_\alpha \delta_{\alpha\beta}, \quad (8)$$

ϵ_α independent of t_z .

For this case we find the lowest four "central" moments are given by

$$\langle E \rangle = (N+Z) \langle \epsilon \rangle, \quad (9a)$$

$$\langle (E - \langle E \rangle)^2 \rangle = \frac{1}{(d-1)} \{ N(d-N) + Z(d-Z) \} S_2, \quad (9b)$$

$$\langle (E - \langle E \rangle)^3 \rangle = \frac{1}{(d-1)(d-2)} \{ N(d-N)(d-2N) + Z(d-Z)(d-2Z) \} S_3, \quad (9c)$$

$$\begin{aligned} \langle (E - \langle E \rangle)^4 \rangle = & \frac{N(d-N)(6N^2 + d^2 - 6Nd + d) + Z(d-Z)(6Z^2 + d^2 - 6Zd + d)}{(d-1)(d-2)(d-3)} S_4 \\ & + \left\{ 3d \frac{N(N-1)(d-N)(d-N-1) + Z(Z-1)(d-Z)(d-Z-1)}{(d-1)(d-2)(d-3)} \right. \\ & \left. + 6 \frac{N(d-N)Z(d-Z)}{(d-1)(d-1)} \right\} (S_2)^2, \end{aligned} \quad (9d)$$

where $\langle \epsilon \rangle$ is the average of the ϵ_α over the active single-neutron or single-proton states

$$\langle \epsilon \rangle \equiv \frac{1}{d} \sum_{\alpha} \epsilon_{\alpha}, \quad (10a)$$

and similarly

$$S_p \equiv \frac{1}{d} \sum_{\alpha} (\epsilon_{\alpha} - \langle \epsilon \rangle)^p. \quad (10b)$$

Furthermore, we use σ , γ , and η to denote the width, skewness, and excess of $\rho(E)$, respectively:

$$\begin{aligned} \sigma & \equiv [\langle (E - \langle E \rangle)^2 \rangle]^{1/2}; \\ \gamma & \equiv \frac{\langle (E - \langle E \rangle)^3 \rangle}{\sigma^3}; \\ \eta & \equiv \frac{\langle (E - \langle E \rangle)^4 \rangle}{\sigma^4}. \end{aligned} \quad (11)$$

Here $\rho(E)$ for the (N, Z) problem is a convolution of the $\rho(E)$ functions for the $(N, 0)$ and $(0, Z)$ problems. As a consequence the p th central moment of $\rho(E)$ for (N, Z) can be assembled from the p th and lower central

moments of the neutrons-only and protons-only distributions. This structure is evident in Eq. (9). In addition, $\rho(E)$ and its moments are unaltered by an interchange of the values of N and Z .

We have investigated a variety of forms for the approximate DOS function, $\rho_a(E)$. We present results for four choices: the truncated Gram-Charlier series using two, three, and four moments; and an inverted Weibull¹² distribution:

$$\rho_a: \begin{cases} \rho_{Gm}(E) = D \frac{\exp(-\frac{1}{2}x^2)}{\sqrt{2\pi}\sigma} \left[1 + \sum_{\mu=2}^m \frac{\gamma_\mu}{\mu!} \text{He}_\mu(x) \right]; & (12a) \\ x = \frac{E - \langle E \rangle}{\sigma}; \quad m = 2, 3, 4; \quad \gamma_2 \equiv 0, \\ \rho_W(E) = \frac{Dc}{-b} \left[\frac{(E-e)}{b} \right]^{c-1} \exp \left[- \left[\frac{(E-e)}{b} \right]^c \right]; \quad E \leq e, \quad b < 0. & (12b) \end{cases}$$

Here, the $\text{He}_\mu(x)$ denote the Hermite polynomials.¹³ The constants $\{\gamma_\mu\}$ in Eq. (12a) are chosen such that $\rho(E)$ and $\rho_{Gm}(E)$ have the first m moments in common. Similarly, $\{b, c, e\}$ of Eq. (12b) are chosen such that the first three moments of ρ_W equal those of ρ . The general Gram-Charlier series can be used to construct a function having an arbitrary number of moments in common with ρ . This useful feature is balanced by the fact that unphysical regions of negative density can occur in $\rho_{Gm}[m \geq 3]$, usually in the tails of the distribution. This motivates the use of alternative ρ_a forms which are guaranteed to be non-negative everywhere. For this reason we include the Weibull distribution which is completely determined by three moments and by the total dimensionality.

For a given choice of ρ_a , an estimate E_a of the PHP g.s. energy for the (N, Z) system is determined by the Ratcliff⁵ condition

$$\int_{-\infty}^{E_a} \rho_a(E) dE = \frac{q}{2}; \quad q = \begin{cases} D_{g.s.}, & \text{if known} \\ 1, & \text{otherwise.} \end{cases} \quad (13)$$

Here $D_{g.s.}$ denotes the degeneracy of the PHP ground state. When $D_{g.s.}$ is unknown, as is the usual case when moment methods are used, $q=1$ is chosen. Note that if ρ_a in Eq. (13) is replaced by the exact (discrete) ρ , E_a is found to equal $E_{g.s.}$ for any choice of q on the interval $0 < q \leq 2D_{g.s.}$. In practice, E_a is determined to the desired precision by numerical integration of ρ_a . When ρ_a has negative regions at small E , we integrate through these regions and beyond until $+\frac{1}{2}q$ is accumulated for the first time.

III. CHARACTERISTICS OF $\rho(E)$ FOR THE MODEL PROBLEM

We now consider the specific problem of treating the harmonic oscillator Hamiltonian using a trun-

ated basis of its own eigenfunctions. That is, we choose H in Eq. (5) to be H_0 itself, and we use

$$\epsilon_\alpha = (N_\alpha + \frac{3}{2}) \hbar\omega$$

in Eq. (10). On one hand we deduce the exact $\rho(E)$ function by enumerating the energies of the D basis states. The calculation of the exact PH_0P ground state energy and its degeneracy is particularly simple. On the other hand, we employ moment methods to generate in turn the S_p averages, the central moments of ρ , the approximate ρ_a functions, and the E_a values. We then investigate the error in the moment-method estimate of the g.s. energy, $E_a - E_{g.s.}$, as a function of (N, Z) , truncation scheme, basis size, and ρ_a form. We confine our numerical calculations to systems near $(N, Z) = (8, 8)$ to facilitate a later comparison⁹ with results for a realistic nuclear Hamiltonian.

The moment method proved much more successful in predicting the H_0 g.s. energy when ETS bases were used, and consequently the bulk of the results displayed herein are for such bases. The interested reader may consult Ref. 14 for a more thorough discussion of STS and ETS results.

Let r denote the largest value of the energy label N_α which occurs for the active single-nucleon states of a given ETS or STS basis. d , $\langle \epsilon \rangle$, and the S_i are found to be¹⁴ simple polynomials in r . The mean, width, skewness, and excess of $\rho(E)$ are then easily calculated from Eq. (9) and (11). σ , γ , and η , regarded as functions of (N, Z) for fixed basis type and size ($d \gg N, Z$), are strongly dependent on $A = N + Z$. For fixed A , each has only a small residual dependence on $N - Z$, and this dependence vanishes as d becomes infinite. For example, under the ETS we find

$$\langle E \rangle \xrightarrow{d \rightarrow \infty} \frac{3}{4}(3d)^{1/3}A \approx 1.082d^{1/3}A, \quad (14a)$$

$$\sigma_{d \rightarrow \infty} \rightarrow \left(\frac{3}{80}\right)^{1/2} (3d)^{1/3} A^{1/2} \approx 0.2793 d^{1/3} A^{1/2}, \quad (14b)$$

$$\gamma_{d \rightarrow \infty} \rightarrow -\left(\frac{80}{3}\right)^{3/2} \frac{1}{160} A^{1/2} \approx -0.8607 A^{-1/2}, \quad (14c)$$

$$\eta_{d \rightarrow \infty} \rightarrow 3 + \frac{0.09524}{A}. \quad (14d)$$

In the dilute system limit ($d, A \rightarrow \infty, A/d \rightarrow 0$) γ and η approach the Gaussian values of 0 and 3, respectively, for either truncation scheme, in agreement with the work of Ginocchio.²

For the $N=Z=8$ system, Fig. 1 displays a histogram constructed from $\rho(E)$ for an ETS basis of moderate dimensionality. Three of the continuous approximations of Eqs. (12) are also shown for comparison. For E_{112} the left-hand tail of $\rho(E)$ on $36\hbar\omega \leq E \leq 40\hbar\omega$ can be considered "physical" in the sense that the eigenstates of H_0 and PH_0P are identical and in one-to-one correspondence there. Thus enlargement of the basis would not affect $\rho(E)$ on this interval. The low-moment constraints force the $\rho(E)$ histogram and its continuous approximations to agree closely in the high density region, but significant differences are often evident elsewhere.

The exact histogram in Fig. 1 has a noticeable negative skewness due to the preponderance of high energy orbitals in the active single-nucleon space. The Gaussian approximation ρ_{G2} , which ignores this skewness, departs significantly from ρ at high energies but is surprisingly near to ρ in the physical region. Using ρ_{G3} improves the agreement substantially for higher energies but does not improve agreement in the physical region.

IV. ERROR IN THE MOMENT-METHOD ESTIMATE OF THE g.s. ENERGY

The problem of accurately estimating the g.s. energy of PH_0P from the low moments of $\rho(E)$ is a formidable one. The physical tail of $\rho(E)$ is only a small contributor to the lower moments, and, for the largest basis (E_{440}), lies eleven standard deviations to the left of the mean. Padé approximants can be used to deduce rigorous upper and lower bounds to $E_{g.s.}$ from the moments of $\rho(E)$, but for large D and few moments these bounds are too wide to be of practical use. For example, rigorous bounds deduced from the first four moments confine the $H_0(N,Z)=(8,8)$ ground state to

$$-4.1 \times 10^6 \leq E_{g.s.} / \hbar\omega \leq 78$$

for the E_{112} basis of Fig. 1. The width of these bounds reflects the fact that there exists a wide variety of non-negative discrete distributions having the same first four moments as $\rho(E)$.

Equation (13) provides an alternative to the rigorous bounding procedures. Its effectiveness is

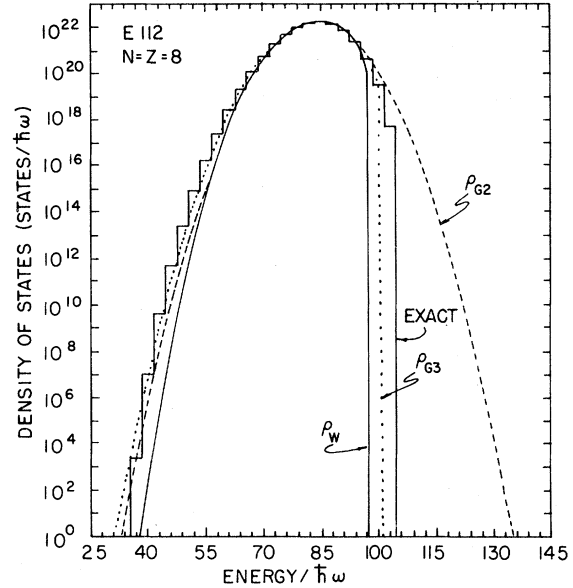


FIG. 1. Comparison of exact and approximate density-of-states functions for the E_{112} harmonic oscillator basis ($N=Z=8$). The histogram representing the exact function $\rho(E)$ has been constructed by partitioning all eigenvalues of PH_0P into bins of width $3\hbar\omega$ centered on $E/\hbar\omega = 37, 40, 43, \dots$. The Gram-Charlier approximation $\rho_{Gm}(E)$ is obtained from the first m moments of $\rho(E)$, while the Weibull distribution $\rho_w(E)$ requires three moments of $\rho(E)$.

dependent on how clearly ρ_a mirrors ρ in the physical region. The choice of the ρ_a function, the basis size and truncation scheme, and the particle numbers (N, Z) all influence the error $E_a - E_{g.s.}$. In this section we examine $E_a - E_{g.s.}$ as a function of these controllable variables for $(N, Z) = (8, 8)$ and neighboring systems.

A. The H_0 problem near $N=Z=8$

The ground state for the $(N, Z) = (8, 8)$ system of H_0 is nondegenerate and has energy $E_{g.s.} = 36\hbar\omega$. The g.s. eigenstate $|\psi_1\rangle = |\phi_1\rangle$ is included in every expansion basis we consider, and the exact g.s. energy consequently appears among the list of PH_0P eigenvalues which determine $\rho(E)$. The error $E_a - E_{g.s.}$ for $(N, Z) = (8, 8)$ is displayed in Fig. 2 as a function of basis dimensionality for both truncation schemes and several choices of ρ_a . ρ_{G4} is negative in the left-hand tail for STS bases, and this fact contributes to the rapid divergence of the corresponding E_a from $E_{g.s.}$. For ETS bases, the left tail of ρ_{G4} is positive and leads to E_a values intermediate to those shown for ρ_{G2} and ρ_{G3} . It is remarkable that one of the simplest calculations, the two-moment Gaussian approximation to $\rho(E)$, leads to one of the least divergent and most accurate estimates of $E_{g.s.}$

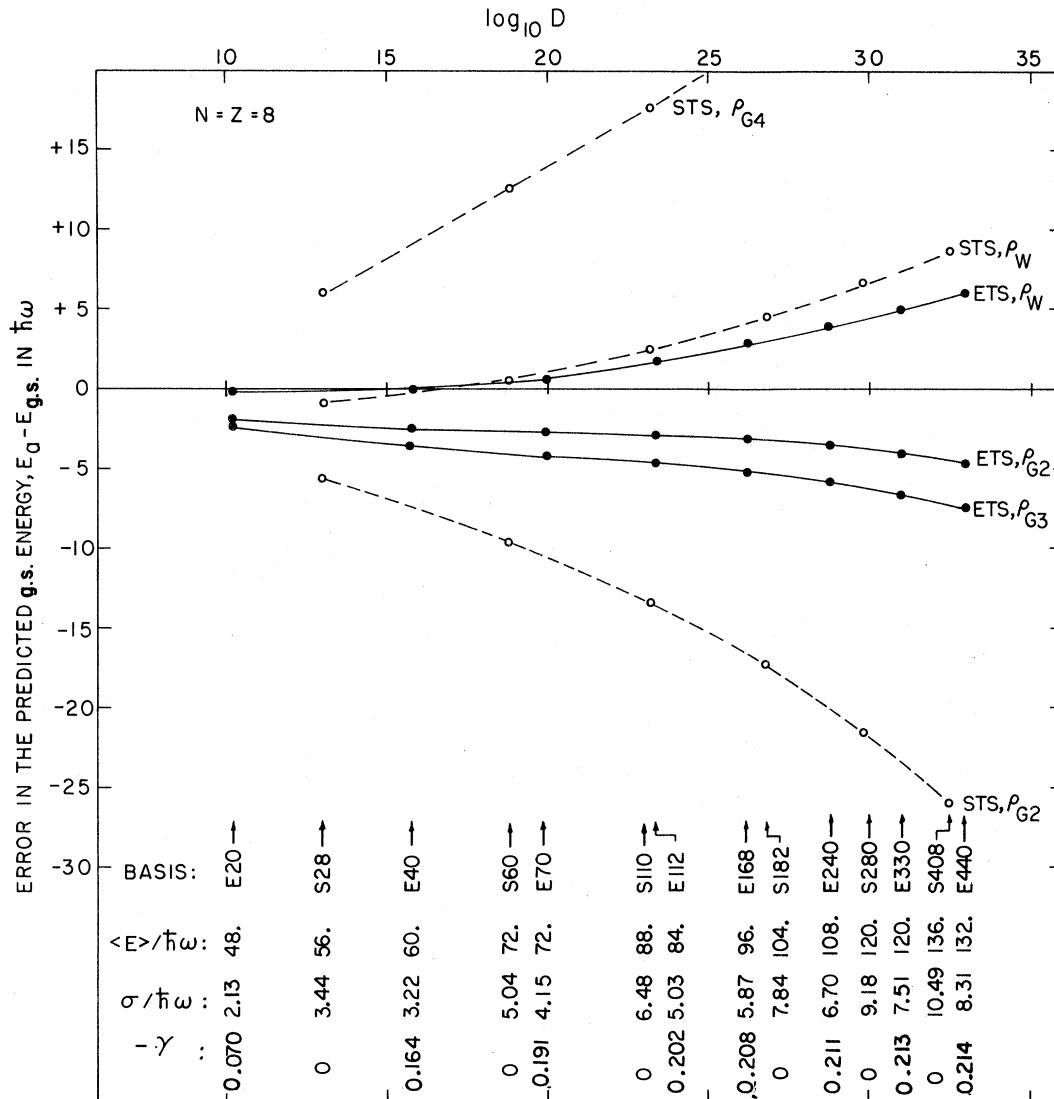


FIG. 2. Error in the moment method estimate of the harmonic oscillator $N=Z=8$ ground state energy. Results are displayed as a function of basis dimensionality for both truncation schemes and for several choices of the continuous DOS approximation $\rho_a(E)$. For each basis the centroid, width, and skewness of the exact $\rho(E)$ are indicated.

Equally remarkable is the rapid divergence of the Gaussian calculation for STS bases. The definition of the STS ensures that $\rho(E)$ for the $H=H_0$ problem is symmetric about its mean, and hence, more nearly Gaussian in appearance than its ETS counterpart. However, only the left-hand tail region contributes to the g.s. energy estimate, and there ρ and ρ_{G2} are most similar for the energy truncated basis. For both ETS and STS bases, the Weibull distribution which requires three moments is seen in Fig. 3 to produce reasonably accurate E_a values over a wide range of dimensionalities.

One strong impression generated from the results of Fig. 2 is the clearly superior performance of the moment method in the ETS over the STS. Another

significant conclusion is the slow growth and smooth behavior of the error as D increases for the ρ_{G2} , ρ_{G3} , and ρ_W choices for the approximate DOS. This smooth behavior suggests a systematic correction procedure might be developed for moment method results with realistic Hamiltonians to improve accuracy.

For nuclei other than $(N,Z)=(8,8)$, one must address the question of which value of q to use in Eq. (13). Since the g.s. degeneracies are quite large for some of the $(8,8)$ neighbors, e.g., $D_{g.s.}=15840$ for $(N,Z)=(13,5)$, the substitution of $q=D_{g.s.}$ for $q=1$ can have a marked effect on the pattern of estimated g.s. energies. This is demonstrated in Fig. 3. Only ρ_W results for $E112$ are shown, but similar modifi-

cations of the g.s. energy pattern occur for the other ρ_a and bases studied when $q=1$ is replaced by $q=D_{g.s.}$ in Eq. (13). In each case $E_a(N,Z)$ is shifted upward relative to $E_a(8,8)$ by an amount which increases with increasing $D_{g.s.}(N,Z)$.

The pattern of exact H_0 energies near $A=16$ possesses several features which are strongly dependent on shell effects. The behavior of $E_{g.s.}$ within an A chain is particularly sensitive to the closed-shell structure of the $N=Z=8$ ground state. A knowledge of the g.s. degeneracy as a function of (N,Z) enables one to reconstruct the shell structure of the H_0 single-nucleon energies. Thus it is not surprising that using $q=D_{g.s.}$ in place of $q=1$ in Eq. (13) leads to a more faithful reproduction of the g.s. energy pattern. In practical applications of moment methods, such detailed knowledge of g.s. properties of H will probably not be available, and hence $q=1$ (or perhaps $q=2$ for odd- A systems) must be used in Eq. (13). However, g.s. degeneracies will be much smaller for realistic nuclear Hamiltonians than for H_0 ; the difference between the $q=1$ and $q=D_{g.s.}$ estimates of the g.s. energy will generally be a fraction of $\hbar\omega$ in realistic cases.

If Fig. 2 were redrawn for a neighboring (N,Z) system, the result would be very similar to the $N=Z=8$ case shown. Consequently, relative g.s. energies predicted by the MM are much more stable to changes in basis dimensionality than are the absolute energies. This point is illustrated more fully in Ref. 14. As one example consider the STS ρ_{G2} cal-

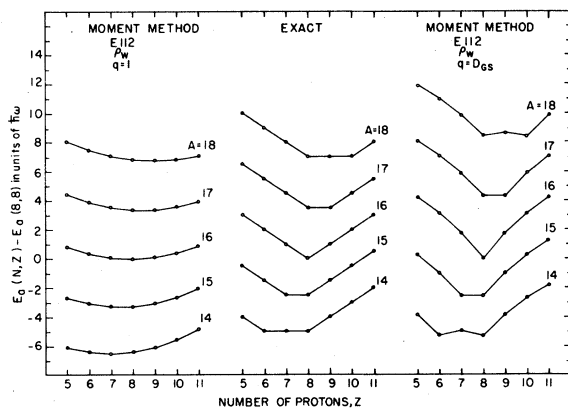


FIG. 3. Patterns of estimated and exact g.s. energies of H_0 for nuclei near $N=Z=8$. The moment-method estimates employ the Weibull distribution and the E_{112} basis. The left and right patterns result from using $q=1$ and $q=D_{g.s.}(N,Z)$, respectively, in Eq. (13) where $D_{g.s.}$ is the exact ground state degeneracy. The exact pattern displays $E_{g.s.}(N,Z) - E_{g.s.}(8,8)$ for the harmonic oscillator problem. The absolute energies of $E_a(8,8)$ and $E_{g.s.}(8,8)$ are $37.6\hbar\omega$ and $36\hbar\omega$, respectively. Each fixed- A curve has reflection symmetry about $Z=A/2$.

ulation, which is one of the more divergent cases in Fig. 2. As we proceed from S_{28} to S_{408} , the predicted g.s. energy of ^{16}O falls by more than $20\hbar\omega$. However, the corresponding predicted ^{18}O - ^{16}O energy difference only changes from $7.5\hbar\omega$ to $6.6\hbar\omega$ for $q=D_{g.s.}$ calculations, and from $5.5\hbar\omega$ to $2.8\hbar\omega$ for $q=1$. (The exact ^{18}O - ^{16}O g.s. energy difference is $7\hbar\omega$ for H_0 .)

Predicted relative energies are generally found to be more accurate and less sensitive to basis size when the ETS is used. Overall, as judged on combined accuracy and stability under basis enlargement, ρ_{G2} and ETS yield the best relative binding energies. However, the three-moment Weibull (ρ_W) results are more accurate for small bases ($d \leq 150$).

When ρ_W is used, ETS and STS bases give similar results at comparable values of d . This is true both for $E_a(8,8)$ and for the pattern of relative g.s. energies. The g.s. energy pattern obtained from ρ_W slowly expands as d increases. For example, the predicted ^{18}O - ^{16}O energy difference which is $6.8\hbar\omega$ in Fig. 3 ($q=1$) becomes $8.5\hbar\omega$ for an E_{440} basis.

For a given truncation scheme and choice of ρ_a , the average energy separation between A chains is more accurately predicted than is the range of g.s. energy variations within a given A chain. This is clearly the case when $q=1$ is used in the Ratcliff procedure, as evidenced by Fig. 3. Since $q=1$ will

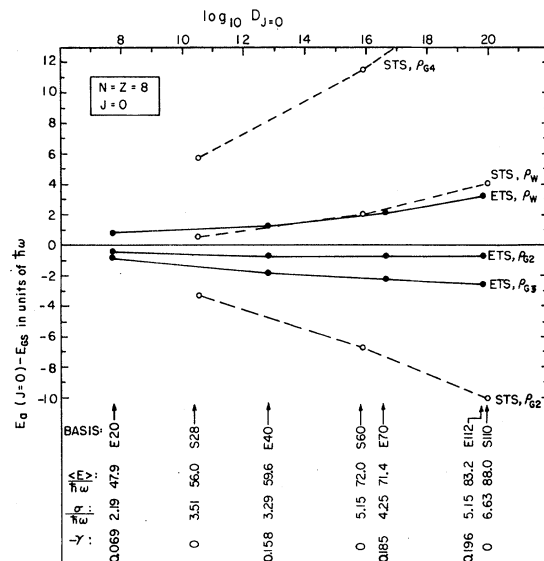


FIG. 4. Error in the moment method estimate of the lowest $J=0$ energy for the H_0 $N=Z=8$ system. Results are shown as a function of basis dimensionality for each of several choices of truncation scheme and ρ_a form. Inputs into the moment method calculations are the lower moments of the exact density of $J=0$ levels, $\rho(J=0, E)$. For each basis, the centroid, width, and skewness of $\rho(0, E)$ is displayed.

be appropriate in moment-method treatments of realistic nuclear Hamiltonians, we anticipate that A -chain separations will again be more accurately predicted in such calculations.

B. Bases of fixed J

Thus far we have used moments of the entire density of states function when estimating the g.s. energy of a Hamiltonian H . As expected, the error in the estimate tends to grow with increasing basis dimensionality D . One way of effectively reducing D is to use a common symmetry of H and the basis Hamiltonian, H_0 , to partition the basis states into sets which are not mixed by H . For example, if H commutes with the square (J^2) and z component (J_z) of the total angular momentum operator, we can choose basis functions

$$\{ |\phi_{JM_i}\rangle; i=1,2,\dots,D_J \}$$

which are simultaneous eigenstates of J^2 , J_z , and H_0 . The diagonalization of the matrix

$$\{ \langle \phi_{JM_i} | H | \phi_{JM_{i'}} \rangle; i,i'=1,2,\dots,D_J \}$$

then determines all simultaneous eigenstates of PHP , J^2 , and J_z . The resulting density of states function $\rho(J,M,E)$ is independent of M , and we use

$$\rho(J,E) \equiv \rho(J,M=J,E)$$

to denote the density of levels of spin J . Thus

$$\rho(E) = \sum_J (2J+1)\rho(J,E); \quad D = \sum_J (2J+1)D_J$$

connect the total density of states and total dimensionality with those of fixed J . The program outlined in Sec. II can be applied to $\rho(J,E)$ to estimate the energy of the lowest level of spin J in the PHP spectrum. This requires the moments of $\rho(J,E)$. In practice these moments can be calculated exactly using the recursive technique of Jacquemin,¹⁵ or approximately using a truncated expansion of $\delta(J_z - M)$.^{7,16}

For the $H=H_0$ problem, $\rho(J,E)$ can be straightforwardly calculated by first enumerating the energies of all fixed- M states in the truncated basis. From $\rho(J,E)$ we then obtain the exact moments as a function of J . We have done this for the $(N,Z)=(8,8)$ system using the ETS and STS bases having $d \leq 112$. For a given ETS or STS basis, the mean, width, skewness, and excess of the total $\rho(E)$ were found to be very similar to those of $\rho(J,E)$ for small J . As an example, $(\langle E \rangle / \hbar\omega, \sigma / \hbar\omega, \gamma, \eta)$ is (84.0, 5.03, -0.202, 2.98) for total $\rho(E)$ in the $E 112$ basis, and (83.2, 5.15, -0.196, 2.97) for $\rho(0,E)$ in the same basis.

The principal difference between $\rho_a(E)$ and $\rho_a(0,E)$ lies in the dimensionality, which is considerably smaller for the latter function, e.g., $D=10^{23.35}$ and $D_0=10^{19.87}$ for $E 112$. Ignoring other differences we observe that when integrating $\rho_a(E)$ and $\rho_a(0,E)$ in Eq. (13), an accumulated area of $\frac{1}{2}$ would be achieved earlier for $\rho_a(E)$. Consequently, $\rho_a(E)$ tends to produce an estimate E_a that is lower than the $E_a(0)$ obtained from $\rho_a(0,E)$. In addition, there are small differences between the moments of $\rho_a(E)$ and $\rho_a(0,E)$ which also contribute to the difference between E_a and $E_a(0)$. When the ρ_a function is non-negative at low energies, the net effect of using the density of $J=0$ levels in place of the total density of states is to shift the H_0 estimated g.s. energy upward.

For H_0 , the g.s. of the $N=Z=8$ system is a non-degenerate $J=0$ level. Figure 4 displays the results of using the low moments of $\rho(0,E)$ to produce an estimate, $E_a(J=0)$, for the energy of the lowest $J=0$ level. $q=1=D_{g.s.}/(2J+1)$ has been used in the fixed- J counterpart to Eq. (13). As in Fig. 2, results are shown for both truncation schemes and for a variety of choices for $\rho_a(J=0,E)$. By comparing Figs. 2 and 4, the restriction to $J=0$ can be seen to shift the predicted g.s. energy upward by roughly 1 to $3\hbar\omega$ for bases with $d \leq 112$. The ρ_{G2} and ρ_{G3} estimates, which are too low in Fig. 2, are thus improved, while the ρ_W estimates worsen. For fixed ρ_a and truncation scheme, the manner and rate at which the estimated g.s. energy diverges from the exact value as the basis dimensionality increases is similar in Figs. 2 and 4.

Moments of the $\rho(J,E)$ distributions can also be used to estimate the lowest energy levels for a sequence of J values. The results of four such calculations for $N=Z=8$ are shown in Fig. 5. For a given basis space, the $\rho(J,E)$ with $J \leq 10$ differ only slightly in their dimensionalities and low-moment characteristics. As a consequence, the resulting estimates $\{E_a(J); J \leq 10\}$ lie within a narrow energy region. This contrasts with the corresponding exact spectrum which extends $3\hbar\omega$ above the $J=0$ ground state. Although there is some overall improvement when the level degeneracies of the exact spectrum are input into the fixed- J counterpart of Eq. (13), the predicted ordering of the levels is poor. We conclude that using a few fixed- J moments will generally lead to the incorrect assignment of the ground state spin. The predicted order of fixed- J levels found here for H_0 resembles the predicted order obtained in ^{16}O moment-method calculations with the realistic effective nuclear Hamiltonians of Ref. 7. This suggests the existence of systematic, J -dependent errors in this type of moment-method prediction of low-lying states.

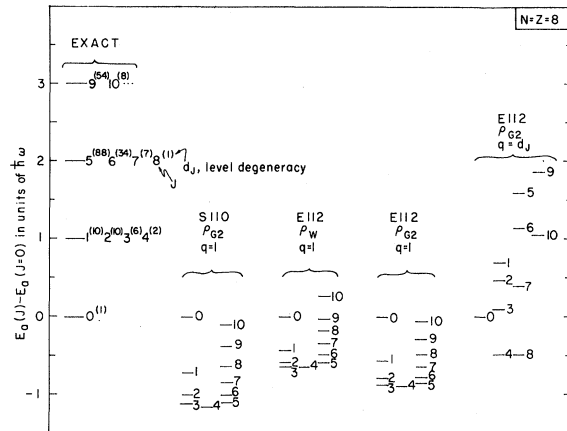


FIG. 5. Lowest energy level of total angular momentum J as predicted by moment methods for $0 \leq J \leq 10$. Results are shown for four choices of calculational ingredients. The harmonic oscillator Hamiltonian ($N=Z=8$) is assumed, and energies are measured relative to the predicted $J=0$ level. For the exact spectrum we also indicate the number of times, d_J , that the minimum-energy J level occurs. These degeneracies were input to the fixed- J counterpart of Eq. (13) for the moment-method calculation depicted at the far right.

V. SUMMARY

In view of the need for developing and testing many-body methods for very large model spaces, we have employed a soluble one-body Hamiltonian, H_0 , to test the ability of moment methods to yield accurate spectral properties of nuclei in the ground state domain. This soluble model retains some significant features of the realistic problem in that the single-particle representation is a conventional harmonic oscillator. We tested the moment method as a function of the size of the model space for two truncation schemes, and for four choices of the smooth approximation, $\rho_a(E)$, to the discrete eigenvalue distribution.

Our most significant finding is that the error in predicting the ground state energy is systematic and increases only slowly with increasing model space size in many cases of interest. The systematic error is different for the varying choices of truncation scheme and of $\rho_a(E)$. Absolute errors are generally less than the width of the total density-of-states function when the conventional energy truncation scheme is used.

The observation of a systematic error and a characteristic dependence on the choice of ingredients for the moment method has two major consequences for applications with realistic Hamiltonians in nuclei. First, *relative* ground state ener-

gies of neighboring nuclei can often be obtained with surprising precision, even when absolute errors are large. Second, the systematic errors documented in the present model calculations may serve as a benchmark for gauging the accuracy of absolute binding energies predicted by moment methods for realistic Hamiltonians. This will be particularly evident if the dependence of predicted g.s. energies upon the calculational ingredients (basis size, truncation scheme, ρ_a form) is found to be similar for H_0 and for the realistic H . Our preliminary calculations with a realistic nuclear Hamiltonian indicate that this is indeed the case. In addition, previously published results for no-core studies with realistic Hamiltonians^{7,8} have employed two moments, the energy truncation scheme (ETS), and the Gaussian choice of $\rho_a(E)$. There, the estimated g.s. energy of ^{16}O was found to be too low when compared with coupled-cluster results,¹⁷ and hence the apparent error is in the same direction as that noted here in the corresponding soluble model calculation. We expect to present elsewhere⁹ more complete moment method results using realistic nuclear Hamiltonians.

There are other points worth noting in the soluble model results. When using only two moments, the optimum results for absolute and relative energies in the ground state domain are achieved using a Gaussian distribution and the conventional ETS. However, we must caution that the exact DOS function was found to possess a sizable skewness for each ETS basis. This skewness is ignored when ρ_a is chosen to be a Gaussian distribution, and the accuracy of moment methods in such circumstances may be in part accidental and peculiar to the soluble Hamiltonian studied. Moreover, our calculations with realistic Hamiltonians find that for a given ETS basis the skewness in the DOS function is even larger in the realistic case than for the corresponding H_0 problem.

Attempts were made to find symmetric truncation schemes for which moment methods provided accurate absolute energies with only two moments. These attempts were not successful. However, with three moments and the Weibull distribution, moment methods produced results of comparable accuracy in the ETS and in a simple symmetric truncation scheme (STS) which we selected for detailed study. The Weibull distribution was selected to cure a significant drawback of the Gram-Charlier (GC) series. For three or more input moments, the GC series yields unphysical regions of negative density of states, whereas the Weibull distribution, which is uniquely determined by three moments, is non-negative everywhere.

We also explored the benefits of using fixed- J densities rather than the total density of states.

Fixed- J bases possess smaller dimensionalities and this tends to decrease the error in the predicted g.s. energy when the g.s. spin is known. In addition, the curves of error versus dimensionality are displaced upward when fixed- J bases are used. This lessens the magnitude of the error in some cases (e.g., ETS with ρ_{G2}) and increases it in others (ETS with ρ_W). In no case were the fixed- J moment-method results accurate enough to correctly predict the ground state spin.

We close with a comment concerning the rise rate of the state density in the ground state domain. With the soluble Hamiltonian the true rate of increase of state density with energy was typically much larger than that of any of the $\rho_a(E)$ forms we explored (e.g., see Fig. 1). Therefore, we argue, more work is needed to develop a better continuous approximation $\rho_a(E)$ that will be useful for predicting both the binding energy of nuclei and the level density in the ground state domain. Alternatively, it

may be worthwhile to explore methods that use the moments of the realistic H in a given space to obtain a soluble H'_0 for the same space with the same first few moments. The level density from such an H'_0 may well be more "realistic" in the g.s. domain than those of the continuous approximations $\rho_a(E)$.

ACKNOWLEDGMENTS

We gratefully acknowledge useful discussions with B. J. Dalton. We thank Thane Doss for showing us that the Weibull distribution would be worthwhile to employ with moment methods. One of us (A.K.) wishes to acknowledge support of the Federal Republic of Germany, Deutscher Akademischer Austauschdienst, and Studienstiftung des deutschen Volkes fellowships. This work was supported by the USDOE, Contract No. W-7405-ENG-82, Division of High Energy, and Nuclear Physics, budget code No. KB-03.

¹F. S. Chang, J. B. French, and T. H. Thio, *Ann. Phys.* (N.Y.) **66**, 137 (1971).

²J. N. Ginocchio, *Phys. Rev. C* **8**, 135 (1973).

³S. Ayik and J. N. Ginocchio, *Nucl. Phys.* **A221**, 285 (1974).

⁴*Theory and Applications of Moment Methods in Many-Fermion Systems*, edited by B. J. Dalton, S. M. Grimes, J. P. Vary, and S. A. Williams (Plenum, New York, 1980), and references cited therein.

⁵K. F. Ratcliff, *Phys. Rev. C* **3**, 117 (1971).

⁶W. Y. Ng and S. S. M. Wong, *Can. J. Phys.* **54**, 2367 (1976).

⁷J. P. Vary, R. Belehrad, and B. J. Dalton, *Nucl. Phys.* **A328**, 526 (1979).

⁸J. P. Vary, see Ref. 4, p. 423.

⁹F. J. Margetan and J. P. Vary, *Phys. Rev. C* (to be published).

lished).

¹⁰J. K. L. MacDonald, *Phys. Rev.* **43**, 830 (1933).

¹¹B. D. Chang and S. S. M. Wong, *Nucl. Phys.* **A294**, 19 (1978).

¹²W. Weibull, *J. Appl. Mech.* **18**, 293 (1951).

¹³M. Abramowitz and I. A. Stegun, *Handbook of Mathematical Functions*, National Bureau of Standards Applied Mathematics Series '55 (U.S. Government Printing Office, Washington, D.C., 1968).

¹⁴F. J. Margetan, A. Klar, and J. P. Vary, Ames Laboratory Report IS-4812, 1982.

¹⁵C. Jacquemin, see Ref. 4, p. 437.

¹⁶J. N. Ginocchio and M. M. Yen, *Nucl. Phys.* **A239**, 365 (1975).

¹⁷H. Kümmel, K. H. Luhrmann, and J. G. Zabolitzky, *Phys. Rep.* **36C**, 1 (1978), and references therein.